ELSEVIER

Atmospheric Research 89 (2008) 161 – 169

ATMOSPHERIC RESEARCH

www.elsevier.com/locate/atmos

Origin of black carbon concentration peaks in Cairo (Egypt)

K.F. Mahmoud [a], S.C. Alfaro [b,*], O. Favez [c], M.M. Abdel Wahab [a], J. Sciare [c]

[a] *Astronomy and Meteorology Department, Faculty of Sciences, University of Cairo, Giza, Egypt*
[b] *LISA, Universités de Paris 12 et Paris 7, CNRS, 61 Av. du Général de Gaulle, 94010, Créteil, France*
[c] *LSCE/IPSL, Laboratoire CEA-CNRS-UVSQ, 91191 Gif/Yvette, France*

Received 5 November 2007; received in revised form 10 January 2008; accepted 10 January 2008

Abstract

The concentration in black carbon (BC) has been monitored in the megacity of Cairo (Egypt) during the autumn 2004 and spring 2005 intensive observation periods of the Cairo Aerosol CHaracterization Experiment (CACHE). As expected for a species released by human activities, hourly mean of this concentration is found to be large at all times. It is also significantly larger in autumn than in spring (9.9±6.6 and 6.9±4.8 μgC/m^3, respectively) and quite variable at shorter (diurnal) time scales. Indeed, sharp concentration peaks larger than 25 μgC/m^3 are frequently detected during both observation periods. In order to apportion the roles played by emission intensity and meteorological conditions in the development of these peaks, a simple model is developed that allows derivation of the hourly mean BC emissions by the part of town located upwind of the measurement site. The analysis of the time dependence of these emissions indicates that traffic is by far the major source of BC in Cairo during daytime and this even in autumn when biomass burning takes place in the Nile delta. It is only between 03:00 and 05:00 in the night, at a time when traffic emissions are quite reduced, that the influence of this particular source on BC concentration can become significant. This study also indicates that BC emissions by motorized traffic remain important from the morning rush hour until late in the night. During the day, and particularly in spring, the dilution effect resulting from the development of the planetary boundary layer prevents BC concentrations from becoming very large. This is no longer the case just before sunrise and after sunset, when the combination of dense traffic and low boundary layer is responsible for the observed sharp increase in BC concentration.

Keywords: Greater Cairo (Egypt); Megacity air pollution; Black cloud; Biomass burning; Black carbon; CACHE

1. Introduction

The population of Cairo has been growing very fast since the 1960s. From approximately 9 millions in 1960, it is now estimated to have reached 16 millions and the intensification of human activities (industry, transport, waste burning…) associated with this population growth most certainly explains the very high pollution levels observed recently in this city (Abu-Allaban et al., 2007; Elminir et al., 2006). The situation is even more critical in autumn and early winter when a dense aerosol plume is present over the city. Because this plume is particularly rich in light-absorbing carbonaceous species (especially black carbon hereinafter referred to as BC) and can therefore be observed with the naked-eye, it has been nicknamed 'Black Cloud' by the city inhabitants. Due to their potential impact on public health, these

* Corresponding author. LISA, Université de Paris 12, 61 Av. du Général de Gaulle, 94010, Créteil, France. Tel.: +33 1 45 17 16 78; fax: +33 1 45 17 15 64.
E-mail address: alfaro@lisa.univ-paris12.fr (S.C. Alfaro).

0169-8095/$ - see front matter © 2008 Elsevier B.V. All rights reserved.
doi:10.1016/j.atmosres.2008.01.004

events are a matter of concern (Sivertsen et al., 2000). In order to help decision makers to define new policies aiming at abating pollution levels, it is first necessary to understand the exact origin of these pollution peaks. The respective roles played by the various sources of carbonaceous aerosols on Black Cloud formation, and especially the effect of the autumnal burning of agricultural residues in the Nile delta, are still unclear. Indeed, in autumn and winter the particularities of local meteorology (lower wind speed and weaker convection than during the rest of the year) could also favor accumulation of aerosols in a shallow planetary boundary layer (PBL) and thus promote Black Cloud formation.

It is the objective of this work to apportion the effects of the various BC sources (listed below) on aerosol concentrations measured at ground level, and this independently of meteorological conditions. For this, the data set collected in a large variety of conditions at Cairo University (Giza) during the two intensive observations periods (IOP1 and IOP2) of the Cairo Aerosol CHaracterization Experiment (CACHE) will be used in combination with local scale meteorological parameters provided by the MM5 model run routinely by the Egyptian Meteorological Authority (EMA).

Practically, the paper is organized as follows. The first section briefly describes the experimental site and proposes a simple modeling approach specially designed for separating the effects of meteorological conditions and of instantaneous emission intensity on BC concentrations. It also details the measurements that are necessary for the application of this model. The second section is a critical analysis of results obtained by the previous method. In particular, emissions intensities are compared for 'usual conditions' and for events of biomass burning advection. Finally, after summarizing the previous findings the last section analyses their implications in terms of potential health hazard mitigation.

2. Methodology

2.1. Experimental site location

A detailed description of the main experimental site selected for the measurements of the CACHE experiments, namely the terraced roof of the physics department on the campus of Cairo University in Giza (lat: N 30°01′33″, long: E 31° 12′ 25″, elevation ca 20 m above ground level), is provided elsewhere in Favez et al. (in press). The city of Cairo itself is located at the southernmost summit of the triangle constituted by the Nile Delta, and Giza Governorate is at the southwest of Cairo conurbation whose shape is rather elongated and oriented along a southwest/northeast axis (Fig. 1). As a consequence of this particular location, it might be expected that, on the one side more pollution from the city itself will be brought to the experimental site when wind blows from the northeast and that, on the other side only winds with directions ranging approximately from northwest (315°) to northeast (45°) will be able to transport biomass burning plumes to the city. Apart from the latter occasions when an external source of carbonaceous (black carbon and organic compounds) species affects concentration levels in Cairo, other sources of BC are either internal or peripheral to the city. These sources correspond to all activities involving incomplete combustion (industries that are numerous within Cairo, ever increasing motorized traffic, outdoor waste burning, street cooking…) and their emissions are expected to be less seasonal than biomass burning.

2.2. Theoretical considerations

A simple box-model can be used to identify the physical parameters that govern aerosol concentrations measured at Giza. Fig. 2 describes the box. It is defined by its location (x) measured along the mean wind direction, its horizontal (dx and dy along and perpendicular to the wind, respectively), and vertical (the PBL height, H) dimensions. Assuming 1) steady state conditions and 2) that wind speed (U) and concentration (C) measured at a fixed height (generally close to 10 m above ground level) are representative of the wind speed and concentration (respectively) averaged over the whole height of the PBL, conservation of the box mass content in any non chemically reactive component

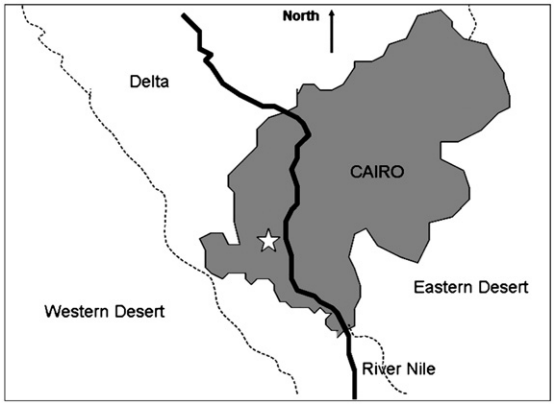

Fig. 1. Map of Greater Cairo with the location of the Cairo University experimental site (white star). The limits of the cultivated Nile delta appear as dashed lines.

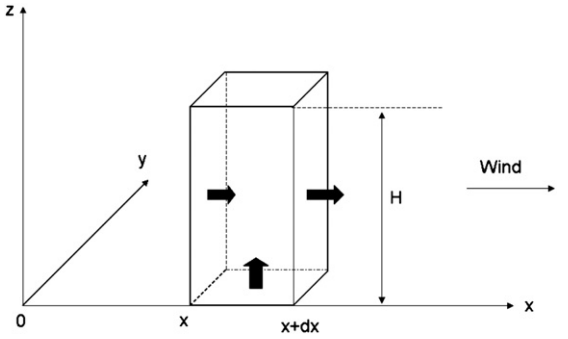

Fig. 2. Scheme of the box used for deriving Eq. (2). The x axis is parallel to the mean wind direction, H stands for the height of the planetary boundary layer, and the black arrows correspond to the incoming and outgoing BC fluxes (see text for details).

leads to the following expression for the dependence of C to x:

$$\frac{\partial C}{\partial x} = \frac{F_S}{UH} \tag{1}$$

In this equation, F_S represents the surface net emission flux for the considered species and can be expressed in $\mu g/m^2/s$, for instance. Its value varies with time according to the fluctuations of source intensities. The product UH is a measure of the dispersing power of the atmosphere and is sometimes used for defining various more or less complex 'ventilation indexes' (Ferguson, 2001). In this paper we will adopt the simplest possible definition for this index, namely the product UH itself. Let us note that this quantity is time-dependent not only because wind speed is not constant but also because of the diurnal variations of H whose value is driven by the amount of solar radiation reaching the ground and absorbed by it.

The local Eq. (1) can be integrated from the upwind limit ($x=0$) of the area containing the sources down to the location of the measurement site (Giza). If we assume spatial homogeneity of UH within this zone and that C is small at the leading edge of Cairo area, this yields:

$$C(x,t) = \frac{1}{UH}\int_0^x F_S dx \tag{2}$$

Finally, if we simply note IF_S the horizontally integrated flux the previous equation can be rewritten as:

$$C(x,t) = \frac{IF_S(x,t)}{UH(t)} \tag{3}$$

This equation confirms that concentration peaks for an inert species produced in the lower troposphere do not necessarily coincide in time with maximal emission. Indeed, relatively weak emissions occurring at times when UH is minimal can lead to large concentration values, and vice versa. More interesting is the fact that Eq. (3) also provides a practical way of assessing time-resolved integrated emissions that are unaffected by the fluctuation of local meteorological parameters. More precisely, these time-resolved emissions can be obtained simply as the product of C and UH provided the time dependence of these two quantities are known.

2.3. Available data

2.3.1. Computation of the meteorological data

The fifth-generation NCAR/Penn State Mesoscale Model (MM5) documented by Anthes and Warner (1978) has been used to calculate the planetary boundary layer height (H) and wind characteristics (direction and speed) at 10 m. For these computations an area with longitude between 10E and 55E and latitude between 10N and 45N and a spatial resolution of 54×54 km have been selected. The NCEP WAFs (initial and boundary conditions every 6 hours) have been used as meteorological input data and the selected computational time step has been fixed at 180 s. In this paper we will only use the hourly averages of U, H, and wind direction.

2.3.2. Experimental results available from CACHE

Most of the CACHE ground level measurements were performed during its two intensive observation periods. The first one (IOP1) was carried out in autumn (from October 29 to November 16, 2004) and the second one in spring (from March 20 to April 13, 2005). These periods had been selected a priori because of the high probability of observing biomass burning episodes during IOP1 and dust events during IOP2. It must be noted that in 2004, most of IOP1 coincided with the Ramadan period. At this time of year Muslims modify their habits to comply with their religious obligations. In particular they go home earlier than usual in the afternoon. They also have a particularly reduced activity in the two days preceding the closure of the Ramadan fasting period. In 2004, these two days were Nov. 12 and 13.

During IOP1 and IOP2, airborne particles were collected on Nuclepore filters (47 mm-diameter 0.4 μm-pore-size Nuclepore AOX) using a sampling line with a 10 μm diameter cut-off. Total numbers of 52 and 103 Nuclepore filters were collected during IOP1 and IOP2 respectively. The content of these filters was submitted to X-Ray Fluorescence analysis for assessing their elemental composition. This technique provides the

possibility (see Alfaro et al., 2003, for a description of the method) of quantifying the concentration in potassium element that is not associated with mineral dust (K_{nd}). The ratio of K_{nd} to BC is a tracer of biomass burning (Gaudichet et al., 1995) that is particularly useful to locate in time the biomass burning events that occurred during IOP1 and possibly during IOP2.

One of the disadvantages of the filter sampling is its poor time resolution. Indeed, the duration of collection for each filter was typically three hours, a value that is not in keeping with the fast evolution of the PBL height especially close to sunrise and sunset. Thus, making the most of Eq. (3) necessitates faster BC measurements than those that can be obtained from filter analysis. These fast measurements are provided by the seven wavelength (370, 470, 520, 590, 660, 880, and 950 nm) aethalometer (Magee Scientific, model AE-42) that was operated during the two IOPs at a time step of 5 min and a flowrate of 5 L mn^{-1}. The original purpose of the instrument was to deduce the spectral absorbing properties of the aerosol from measurement of the attenuation of light caused by atmospheric particles when they are progressively accumulated on a fiber filter (Hansen et al., 1982). At 660 nm, BC particles could be assumed to be the only light absorber, as neither mineral dust nor organic compounds found in Cairo atmosphere absorb at this wavelength (Alfaro and Abdel Wahab, 2006). The 660 nm wavelength channel was thus chosen in this study to investigate black carbon particles. Practically, BC mass concentration were retrieved from light absorption coefficient measurement using the standard conversion factor, also called mass absorption efficiency (MAE), of 22.2 g/m^2 given by the manufacturer. Noteworthy, MAE was found to vary with aerosol sources (industrial or biomass burning combustion) and aerosol aging (Liousse et al., 1993). However, BC thermo-optical measurements performed on quartz fiber filter (47-mm diameter Whatman QMA) samples – using a OC-EC Lab Instrument from Sunset Lab., Forest Groove, OR– were found to correlate successfully with aethalometer absorption coefficient measurements ($r^2=0.96$, $n=12$) during IOP1, when both biomass burning and industrial combustion are expected to affect Cairo atmosphere. An average MAE value of 23.1 ± 2.6 m^2/g was obtained from this inter-comparison exercise, which is consistent with the 22.2 m^2/g MAE value used in this study. Measurements performed every 5 min at 660 nm wavelength are used to compute BC hourly means for the whole durations of IOP1 and IOP2.

In summary, the MM5 model outputs and the aethalometer measurements provide the data necessary for determining from Eq. (3) the integrated emission fluxes at a regular, hourly time step.

3. Results and comments

3.1. Comparing general conditions for the two measurement periods

3.1.1. Local meteorology

Examination of the distribution of surface wind directions computed with the MM5 model (Fig. 3) reveals that north to northeastern winds prevailed during IOP1 and IOP2. In both cases, approximately 55% of wind directions were between 0 and 90° that is to say in a sector that was most favorable to advection of Great Cairo pollution towards the Giza measurement site. The probability of wind blowing in the 315–45° sector, that is to say from the Nile delta and thus being potentially able to bring biomass burning plumes to the city, is the same during IOP1.

Unlike wind direction, average wind speed was significantly larger (4.0 ± 1.7 m/s) during IOP2 than

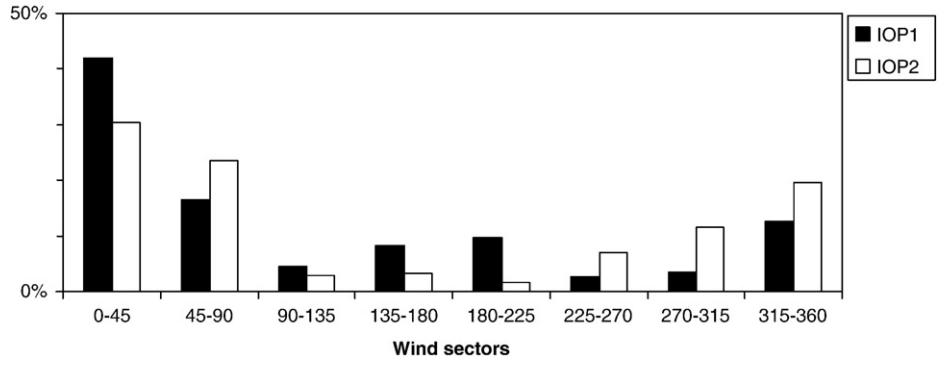

Fig. 3. Distribution of wind direction by sectors for the autumn (IOP1) and spring (IOP2) intensive observation periods of the Cairo Aerosol Charaterization Experiment. Note that wind direction increases clockwise from the north (0°).

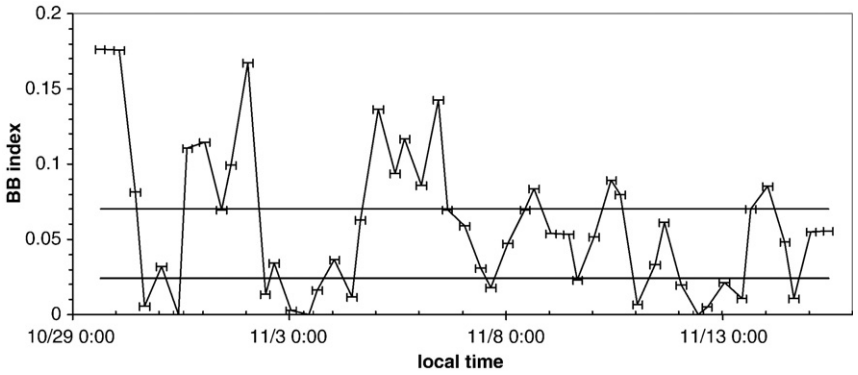

Fig. 4. Temporal localization of the biomass burning events occurring during the first intensive observation period of the Cairo Aerosol Characterization Experiment by the means of the biomass burning index (BBindex). This index is defined as the ratio of potassium not associated with mineral dust to the black carbon concentration. As detailed in the text, biomass burning episodes correspond to values of this index larger than 0.07 (thin line). The horizontal bold line represents the average value of BBindex for the spring observation period when there was no biomass burning.

during IOP1 (3.1±1.2 m/s). It can be noted that this difference is in fact mostly due to 3 relatively short periods of strong southwestern winds in the spring period that also corresponded to events of mineral dust advection to Cairo. In addition to this wind speed difference, and though average PBL heights were quite similar between IOP1 and IOP2 (820±820 m vs 880±770 m, respectively), a better temporal coincidence of wind speed and PBL height maxima during the second period produced much larger values of midday ventilation index in spring than in autumn. This is reflected by the period averages (4100±5200 for IOP2 as compared to 2100±2900 m^2/s only for IOP1).

3.1.2. Concentration and origin of carbonaceous species

As expected for a polluted megacity, black carbon concentrations measured at ground level and averaged over the whole duration of IOP1 and IOP2 are large in both cases, though significantly different (9.9±6.6 and 6.9±4.8 $\mu gC/m^3$, respectively). Also noteworthy is that the order of magnitude of these large concentration values is in good agreement with those also obtained in downtown Cairo by Abu-Allaban et al. (2007).

In order to assess the part played by biomass burning in the IOP1/IOP2 difference, the biomass burning index (BBindex = K_{nd}/BC) defined above has been used to locate in time potential advection of biomass burning

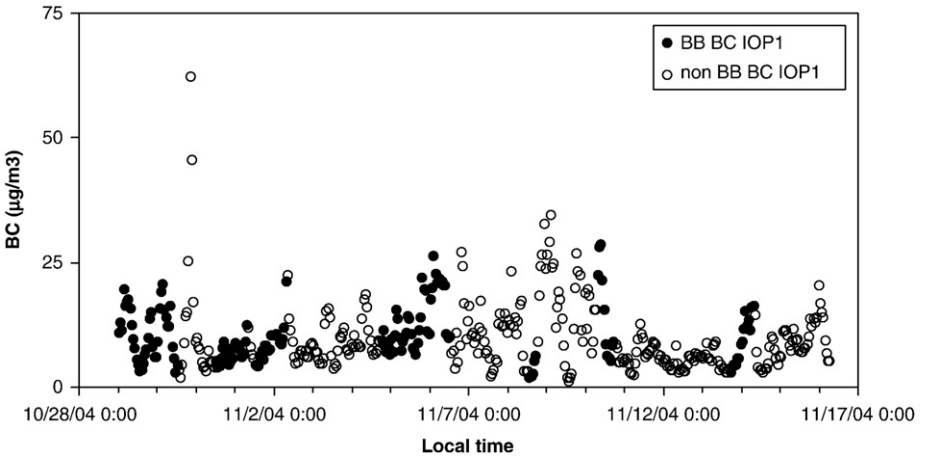

Fig. 5. Hourly averages of the Black carbon concentration measured at ground level during the first intensive observation period (IOP1) of CACHE. These averages are computed from the aethalometer data acquired at a 5 min time step. For the sake of comparison measurements performed in periods of biomass burning (black circles) have been distinguished from the others (open circles).

plume during IOP1. Prior to this, the index has also been calculated for IOP2 in order to determine its reference value for non biomass burning situations. The average and associated standard deviation found for IOP2 are BBindex = 0.024 (±0.023). We will consider hereinafter that this value corresponds to 'business as usual' (non biomass burning) activities in Greater Cairo and that any significant increase above this threshold traces biomass burning activities. Practically, a BBindex > 0.07 (average + 2 standard deviations) has been retained as a numerical criterion for defining periods influenced by biomass burning. When applied to IOP1, this method shows that several biomass burning periods occurred during the fall CACHE measurements (Fig. 4). Though results are not shown here, it has also been checked that – during these periods – wind was always blowing from the Nile delta, which is to say in the 315–45° direction sector.

It is now possible to distinguish between the IOP1 BC measurements made in biomass and non biomass burning conditions. Fig. 5 does not reveal any obvious difference between the two kinds of periods, which is confirmed by the computation of the BC averages and standard deviations for the BB and non BB conditions, (10.6 ± 5.7 as compared to 9.6 ± 6.9 μg/m^3, respectively). This first result indicates that the occurrence of biomass burning alone can not account for the large peaks of BC concentration observed at ground level in Cairo.

3.1.3. Influence of ventilation index on BC concentration

Eq. (3) shows that fluctuations in ventilation index (UH) could also explain BC peaks. Fig. 6 confirms that an increase in UH tends to reduce BC concentrations measured at ground level during IOP1 and IOP2, but the relationship between UH and BC is far from being unequivocal. Indeed, except at very large UH values for which measurements are relatively scarce, the range of measured BC concentrations for each UH value spans at least one order of magnitude. The explanation for this very large variability probably lies in the fact that the horizontally integrated emission flux appearing in Eq. (3) depends on the time of day and possibly also on wind direction. The next section examines these dependences first during IOP2 that was closest to 'business as usual' conditions (this was not Ramadan period and there was no biomass burning) then during IOP1.

3.2. Time-resolved integrated emission flux during IOP2

The hourly averages of IFS computed for the 0–90° wind directions of IOP2 are plotted against time on Fig. 7. It shows that the integrated emissions for sources of BC located upwind of the experimental site vary by one order of magnitude between the small hours of the day (between 3 and 5 AM) when emissions are minimal and a relatively flat maximum observed between approximately 8 AM and 4 PM). The morning transition from the night minimum and the plateau occurs between 6 and 8 AM, which is to say at the time of the morning traffic peak. The evening decrease in BC emissions is much slower and it is not before 2 AM that they retrieve their nocturnal minimal value. This is also in good agreement with direct observations showing that traffic in Greater Cairo is always rather dense except very late in the night. This good correspondence between the IF_S

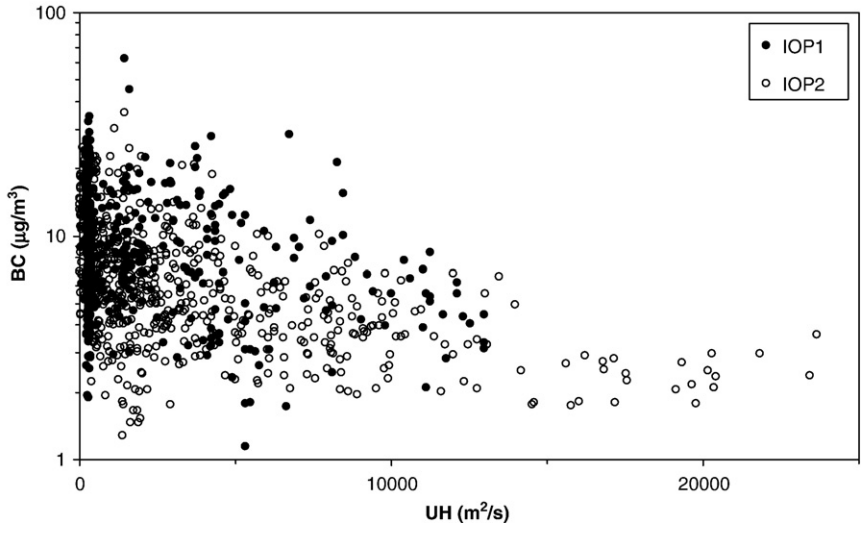

Fig. 6. Influence of the ventilation index (UH) on the black carbon concentrations measured at ground level during the autumn (IOP1) and spring (IOP2) intensive observation periods of CACHE.

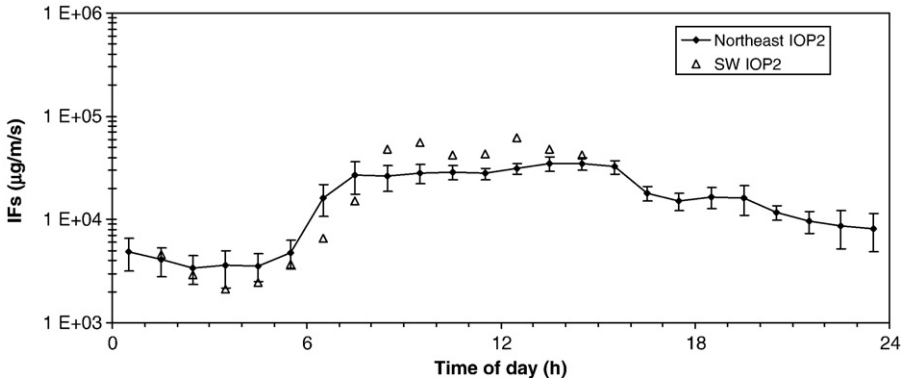

Fig. 7. Dependence on the hour of day of the BC surface emissions during IOP2. These emissions are integrated horizontally along the wind direction from the upwind leading edge of Greater Cairo to the location of the measurement site. Our results show that the integrated flux depends greatly on the time of day but not significantly on wind direction (compare results obtained for northeastern winds to southwestern ones).

diurnal cycle and that of traffic tends to indicate that, at least during non biomass burning periods and with the possible exception of late night, emission of BC by car engines dominate all other potential sources in Cairo. This conclusion does not seem to be challenged when wind blows from other directions than north-east. Indeed, Fig. 7 shows that, at least when experimental data exist for the southwestern direction (i.e. only before 3 PM), the retrieved behavior of IF_S is quite similar in shape and in amplitude to the one already obtained for northeastern winds.

3.3. Time-resolved integrated emission flux during IOP1

When the hourly values of IF_s retrieved for IOP1 under northeastern wind and non biomass burning conditions are plotted against time (Fig. 8) a general shape, quite similar to the one of IOP2, is obtained. This commonality probably indicates that motorized traffic is also the dominant BC source during IOP1, at least in absence of biomass burning. The main difference between the fall and spring periods is that the morning – and most particularly the evening – rush hours no longer occur at the same hours of day during IOP1. Indeed, during Ramadan people tend to go to work later than usual, leave their working places earlier, and not to circulate much after going home (between 16:00 and 17:00). Thus, after 18:00 integrated emissions are quite low, just two or three times larger than the late night minimum, whereas they can become as large as 100 times this value between 10:00 and 11:00. This regular Ramadan day behavior can be compared with the particularly low emissions of November 12 and 13, 2004 (Fig. 8). As already mentioned above, these days coincided with the last two days of the Ramadan fasting

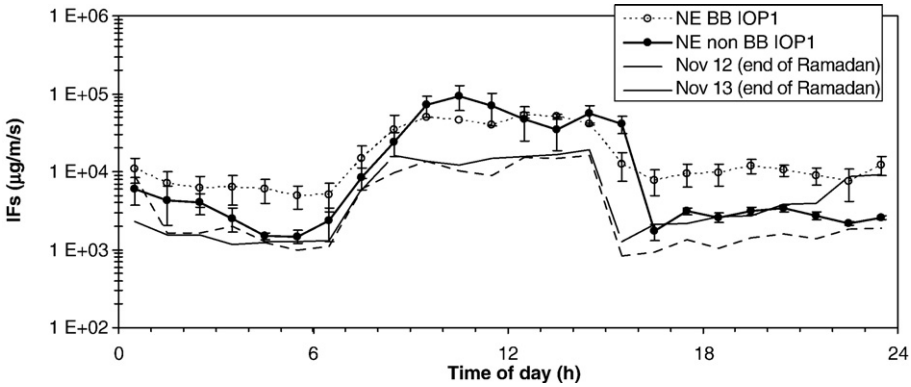

Fig. 8. Same as in Fig. 7 but for the autumn observation period (IOP1). All the results shown correspond to northeastern winds, but biomass burning (NE BB IOP1) and non biomass burning (NE non BB IOP1) cases have been distinguished. For the sake of comparison with 'regular emission' days, results for the last two days of the Ramadan period have also been represented (Nov. 12 and Nov. 13, 2004).

period, a time when activity is traditionally quite reduced, and integrated emissions for these two days most probably constitute the bottom line IF_s of non biomass burning emissions in Greater Cairo. It can be noted that even on ordinary Ramadan days traffic is reduced enough between 04:00 and 06:00 for emissions to reach this bottom line (ca. 10^3 μg/m/s) but that they are from two to ten times larger during the rest of the day. Also noteworthy is that during IOP2 traffic emissions never became as low as the Nov. 13 minimum and this even during the late night emission minimum (see Fig. 7).

Advection of biomass burning plumes can alter this scheme significantly especially at times of reduced traffic. Indeed, our measurements show that between 04:00 and 06:00 integrated emissions incorporating a biomass burning component are 4 to 8 times those (10^3 μg/m/s) of ordinary Ramadan days (Fig. 8). This means that the order of magnitude of the average contribution of biomass burning to total integrated emissions is about 6 ± 2 10^3 μg/m/s for the biomass burning days of the period of study. If we assume that this contribution is relatively constant during the day, it can be considered as small (between 5 and 10%) when compared to daytime traffic emissions. In turn, this weak contribution to daytime overall emissions could explain why non biomass burning and biomass burning plots on Fig. 8 are so similar in amplitude between 08:00 and 16:00.

4. Concluding remarks

It results from the previous analysis that the integrated emission flux can always be considered as a sum of the following potential contributions: background emissions (IF_0), biomass burning (IF_{BB}) that is only occasional, and traffic (IF_{traf}). An additional term (IF_{PS}) could also be added to this list in order to account for the possibility of having an active point source (chimney stack ...) directly upwind of the measurement site, which was the case on the evening of October 30, 2004, when BC concentration peaked at more than 60 μg/m^3 (Fig. 5) due to a building that could be seen on fire in the distance. This leads to the following expression of the integrated flux:

$$IF_s = IF_0 + IF_{BB} + IF_{\text{traf}}(+IF_{PS}) \quad (4)$$

If we exclude the effect of point sources that is by nature hardly predictable, the order of magnitude of the first three terms in Eq. (4) greatly depends on the period of year and time of day. IF_0 is more or less constant and its value is close to 4 ± 3 10^3 μg/m/s, IF_{BB} is by definition nil during non biomass burning periods or when corresponding plumes are not transported to Cairo. Its average value for the biomass burning events of IOP1 is close to 6 10^3 μg/m/s. As for the traffic term, it can be expressed as the product of an amplitude term (between 50 and 100 10^3 μg/m/s) and of a non-dimensional function, $f(t)$, describing its diurnal cycle. Our results have shown that the shape of $f(t)$ is not the same during 'business as usual periods' and during the Ramadan period. Finally, the equivalent of Eq. (3) for black carbon, and without the point-source term, can be rewritten as:

$$BC(x,t) = \frac{IF_0 + IF_{BB}}{UH(t)} + \frac{Af(t)}{UH(t)} \quad (5)$$

A comparison of the orders of magnitude of IF_0 and IF_{BB} on the one side, and A on the other side, immediately shows that during the day the contribution of car traffic to BC concentrations will always be dominant in Cairo even in times of biomass burning. It is only during the night, that is to say when $f(t)$ is very low, that biomass burning can contribute significantly to BC concentrations. Since this is the time when UH is also at its lowest, the corresponding concentrations can reach very high levels in spite of reduced traffic.

Another aspect of biomass burning aerosols that has not been studied in this paper is that they are richer in organic compounds than those produced by combustion in car engines (Novakov et al., 2005). This is particularly true for particles emitted in the combustion of rice straw, which is the main source of biomass burning aerosols during the autumn season in Cairo (Hays et al., 2005). Therefore, the contribution of biomass burning aerosol to the total amount of carbonaceous particles is thus expected to be greater than the one derived by examining the black carbon concentrations only, (Favez et al., in press).

Eq. (3) also provides some clues for abating pollution levels in Cairo. Obviously, the first measure to take would consist in trying to keep all emissions drastically low and at all times, which is not realistic. This is also unnecessary around the middle of the day when UH is large enough to disperse pollution efficiently. On the contrary, reducing emissions becomes crucial between sunset and sunrise when the ventilation index is much lower. Indeed, our result show that during this period the combination of two factors explains the occurrence of BC peaks: the first one is pre-dawn and post-sunset emissions by dense traffic. Promoting the development of efficient public transport and enticing car-owners into

replacing their old cars by cleaner ones could reduce these morning and evening pollution peaks. The second cause is the occasional presence during the night of biomass burning aerosols. Though Egyptian law currently bans outdoor burning of agricultural waste, it is common knowledge that some farmers still get rid of their agricultural residues by setting them on fire just before the night. For mitigating pollution levels in Cairo, it might be more efficient to allow them practice this activity but at different hours to 1) favor initial dispersion within the boundary layer and 2) avoid arrival of the plume over Cairo in the nighttime when even small quantities of additional pollutants can be responsible for a dramatic increase in their concentration.

Acknowledgments

This work has been funded in part by the Egyptian Academy of Sciences and the French Ministry of Foreign Affairs in the frame of the Imhotep program (contract 446538E). The French partners have also benefited from the financial support of the Institut National des Sciences de l'Univers (INSU).

References

Abu-Allaban, M., Lowenthal, D.H., Gertler, A.W., Labib, M., 2007. Sources of PM_{10} and $PM_{2.5}$ in Cairo's ambient air. Environmental Monitoring and Assessment 133, 417–425.

Alfaro, S.C., Gaudichet, A., Rajot, J.L., Gomes, L., Maillé, M., Cachier, H., 2003. Variability of aerosol size resolved composition at an Indian coastal site during the INDOEX intensive field phase. Journal of Geophysical Research 108 (D8). doi:10.1029/2002JD002645.

Alfaro, S.C., Abdel Wahab, M., 2006. Extreme variability of aerosol optical properties: the Cairo Aerosol Characterization Experiment case study. In: Perrin, A., et al. (Ed.), Remote sensing of the atmosphere foe environment security. Springer Verlag, The Netherlands, pp. 285–299.

Anthes, R.A., Warner, T.T., 1978. Development of hydrodynamic models suitable for air pollution and other mesometeorological studies. Monthly Weather Review 106, 1045–1078.

Elminir, H.K., Hamid, R.H., El-Hussainy, F., Ghitas, A.E., Beheary, M.E., Abdel-Moneim, K.M., 2006. The relative influence of anthropogenic air pollutants on the atmospheric turbidity factors measured at an urban monitoring station. Science of the Total Environment 368, 732–743.

Favez, O., Cachier, H., Sciare, J., Alfaro, S.C., El-Araby, T.M., Harhash, M.A., Abdel Wahab, M.M., in press. Seasonality of major aerosol species and their transformations in Cairo megacity. Atmospheric Environment. doi:10.1016/j.atmosenv.2007.10.081.

Ferguson, S.A., 2001. Real-time mesoscale model forecasts for fire and smoke management: 2001. proceedings of the Fourth Symposium on Fire and Forest Meteorology. American Meteorology Society, Botson, MA, pp. 162–167.

Gaudichet, A., Echalar, F., Chatenet, B., Quisefit, J.P., Malingre, G., 1995. Trace elements in tropical African savanna biomass burning aerosols. Journal of Atmospheric Chemistry 22, 19–39.

Hansen, A.D.A., Rosen, H., Novakov, T., 1982. Real-time measurement of the absorption coefficient of aerosol particles. Applied Optics 21, 3060–3062.

Hays, M.D., Fine, P.M., Geron, C.D., Kleeman, M.J., Gullett, B.K., 2005. Open burning of agricultural biomass: physical and chemical properties of particle-phase emissions. Atmospheric environment 39, 6747–6764.

Liousse, C., Cachier, H., Jennings, S.G., 1993. Optical and thermal measurements of black carbon aerosol content in different environments: variation of the specific attenuation cross-section, sigma (σ). Atmospheric Environment 27 (A), 1203–1211.

Novakov, T., Menon, S., Kirchstetter, T.W., Koch, D., Hansen, J.E., 2005. Aerosols organic carbon to black carbon ratios: analysis of published data and implications for climate forcing. Journal of Geophysical Research 110 (D21205). doi:10.1029/2005JD005977.

Sivertsen, B., Ahmed, H.A., Ahmed, H.F., Ahmed, M.E., 2000. A study of air pollutants during episodes. ICEHM2000. Cairo University, Egypt, pp. 345–361.